

The geophysical study of Drybones kimberlite using 3D Time Domain EM Inversion and 3D ZTEM inversion algorithms

Vlad Kaminski

UBC-Geophysical Inversion Facility
6339 Stores Road,
Vancouver, BC, V6T1Z4
vkaminski@eos.ubc.ca

Douglas Oldenburg

UBC-Geophysical Inversion Facility
6339 Stores Road,
Vancouver, BC, V6T1Z4
doug@eos.ubc.ca

SUMMARY

Two airborne EM surveys were conducted over the Drybones kimberlite, NWT, Canada. A VTEM helicopter time domain EM survey was flown by Geotech in 2005, followed by a ZTEM helicopter tipper EM survey flown in 2009. The data sets collected over the kimberlite were inverted and interpreted first by Geotech, Ltd using a 1D TDEM conductivity-depth transform for VTEM data and a 2D inversion for ZTEM data. The data sets were transferred to UBC-GIF for 3D inversions and comparative analysis. Both the VTEM and ZTEM data have now been inverted in 3D and the results compared with the drill data over the kimberlite and with older results of previous geophysical interpretation. The 2D and 3D ZTEM inversions show the same general structure but the 3D inversion has greater electrical conductivity contrast and may have fewer artefacts in zones of low sensitivity. On a large scale the conductivity structure, recovered from the 3D inversion of time domain data, is comparable to that from the CDI transform, but the 3D result shows a more complicated distribution of the conductive properties. The 3D magnetic inversion had not been done previously and it shows susceptible material to depths of approximately 400 m, which is consistent with the known geometry of the kimberlite.

Keywords: 3D inversion, TDEM, ZTEM, kimberlite, airborne

GEOLOGICAL SETTING

The Drybones kimberlite is located approximately 45 km SE from the town of Yellowknife, NWT, Canada (Figure 1A). The bedrock geology in Drybones area consists of Archean granite, granodiorite and tonalite (Kretchmar, 1995). The kimberlite is located on the geological contact between granodiorites and metasediments (schists) of Yellowknife supergroup (Dunn et al., 2001). In addition there are several known tectonic faults present in direct vicinity of the kimberlite. A diabase dike propagates in the E-W direction across the area under study (Figure 1B).

Drybones kimberlite lies completely underwater, at an average depth of 38 m. It is further overlain by 65-75 m of lake sediments, predominantly clay, till and sand (Figure 1C). The

morphology of the pipe can be described as a spatially elongated intrusion (900 m by 400 m), consisting of three main facies (diatreme, crater and pyroclastic) distinguished by physical and mineralogical properties of the rock. The level of consolidation of the kimberlite varies between different facies, which is expected to be reflected in the electrical properties of the kimberlite (greater consolidation corresponds to higher electrical resistivity values).

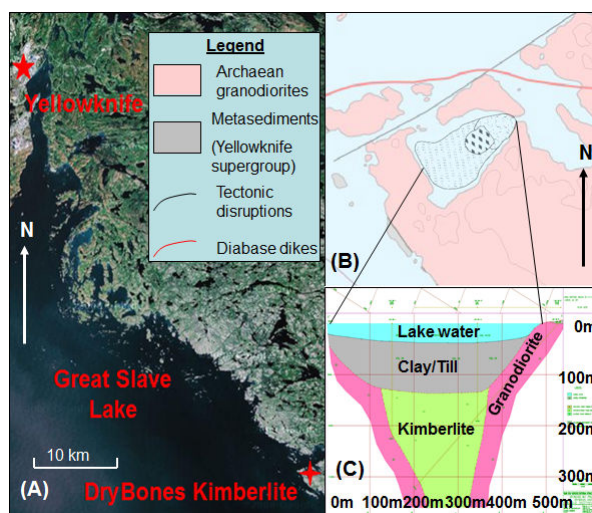


Figure 1. Location and geology of Drybones kimberlite. (a): Geographic location; (b): Contours of the kimberlite facies; (c): Drybones kimberlite in the cross-section.

The mineralogical analysis of the Drybones kimberlite samples reveals signs of alteration due to elevated contents of Cr and Nb, as well as due to low totals of TiO₂ in ilmenites (Dunn et al, 2001). The geochemical alteration may be reflective in the magnetic properties of the kimberlite.

GEOPHYSICAL SURVEYS OVER DRYBONES

Numerous geophysical studies have been performed over Drybones kimberlite since 1994, including total field magnetic surveys, gravity surveys, VTEM and ZTEM surveys (Kaminski et al, 2010). In this study we are focusing on geophysical surveys flown by Geotech, Ltd from 2005 to 2009, which include two airborne EM studies (VTEM and ZTEM) each accompanied by total magnetic intensity study. In particular, our main emphasis is on 3D inversions which

include inversion of magnetic data, ZTEM data and TDEM data.

3D INVERSION OF MAGNETIC DATA

Total magnetic intensity data were to recover magnetic susceptibility from the 2525 IGRF-corrected magnetic data, flown in tandem with the ZTEM survey. Data were collected with a cesium vapor magnetic sensor flown at the altitude of 60 meters above ground.

The 3D region used for the inversion of magnetic data has been discretized onto 620,136 cells mesh, centered around the core region inclusive of the kimberlite pipe. The core region of the mesh is composed of blocks 25x25x10 meters in size. The maximum depth of the core region reaches 660 meters. The data have been assigned standard deviations of 3nT and inverted using depth weighting (Li and Oldenburg, 1996). The inversion showed convergence to desired misfit (2525) in 4 iterations.

Figure 2 shows depth slices of the recovered magnetic susceptibility plotted over the known contours of the Kimberlite pipe. Elongated magnetic structure in the northern part corresponds to known diabase unit and the kimberlite material shows magnetic signature to depth of 300 m. Figure 3 shows geological depth sections AA' and BB' matched with recovered distribution of the susceptible material. The high susceptibility material associated with the kimberlite is observed to be well differentiated from non-magnetic sediments and this boundary seems to be consistent in all directions. It is possible that the kimberlite material is present at depths greater than 300m, and the magnetically susceptible material only marks that portion of kimberlite, subject to geochemical alteration.

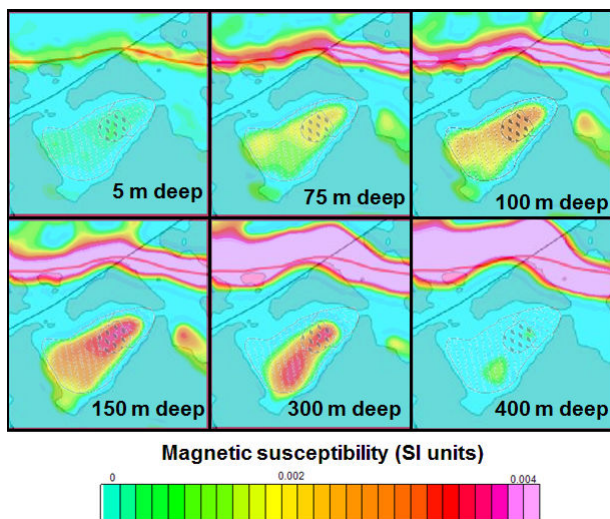


Figure 2. Recovered magnetic susceptibility over Drybones kimberlite overlain with geologic unit contours and presented as a series of depth slices at 5, 75, 100, 150, 300 and 400 m below surface.

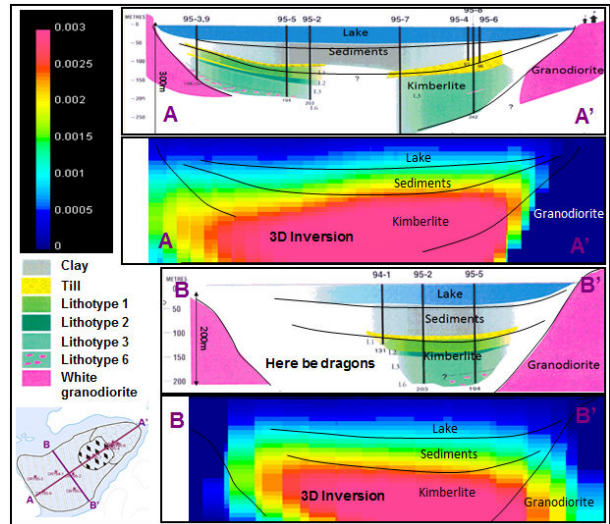


Figure 3. Geological cross-sections based on drilling compared to the magnetic susceptibility model recovered by 3D inversion. For details regarding kimberlite lithotypes refer to (Kretchmar, 1995).

3D INVERSION OF VTEM DATA

Time domain EM data were collected by a VTEM system in 2005. More detailed description of the survey can be found in (Kaminski et al, 2010). The data were inverted using UBC-GIF multi-transmitter 3D time domain inversion code H3DTD (Oldenburg, Haber and Shekhtman, 2011).

The inversion code uses a time-stepping and both the on-time and off-time portions of the waveform are discretised into time segments in which the step interval is a constant. Efficiency of the code in handling multi-transmitters is achieved by decomposing the Maxwell forward modelling matrix. One decomposition is required for each time segment. The discretised waveform is shown in figure 4 and was designed to accommodate 10 time gates, covering the interval from 190 to 1900 μ s with at least one discrete step per time gate..

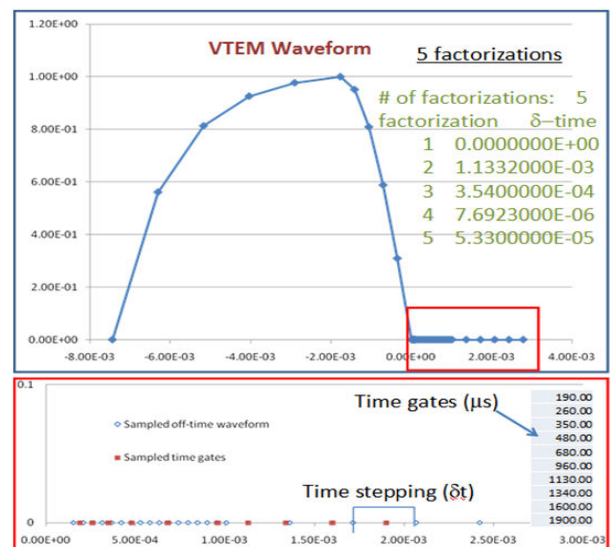


Figure 4. VTEM waveform discretised for H3DTD time-stepping computations.

An initial (coarse) inversion was done on a 156,604 cell mesh consisting of core region and an outer padding area. The smallest cell in the core region measured at 50x50x15m. The data set was sub-sampled to 76 transmitters. This was followed by another 3D TDEM inversion on a refined 252,450 cell mesh (smallest cell: 20x20x7m), centred exactly on the kimberlite, and using 176 transmitters.

The preliminary (coarse) inversion was terminated after 17 iterations and the misfit was 2.058×10^5 . A total of 43 parallelized Intel Xeon processors were employed for the inversion. The following refined inversion was performed using 52 parallelized processors and after 14 iterations achieved a final misfit of 3.82×10^4 . The total number of cells 7.3×10^5 . The data fit for selected VTEM stations and the convergence curves are shown in figure 5.

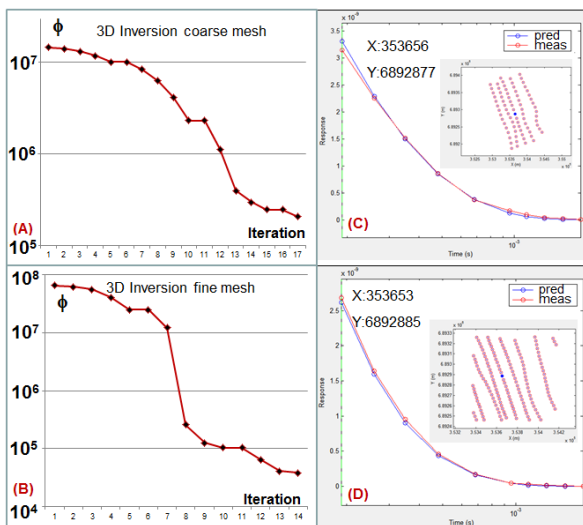


Figure 5. Convergence of two 3D VTEM inversions. (a): Convergence curve for preliminary (coarse) inversion; (b): Convergence curve for refined inversion; (c): Observed versus predicted data for 10 time gates shown at selected location for preliminary (coarse) inversion; (d): Observed versus predicted data for 10 time gates shown at same location as (c) for the refined inversion.

The conductivity models recovered from both inversions were verified against the known geology. This comparison over selected cross-section (AA') is shown in figure 6.

The recovered conductivity values range from 20 Ohm m to 10,000 Ohm m. This is consistent with the anticipated values and fits well with previously done conductivity-depth transforms (Kaminski et al, 2010). In figure 6 it is shown how the fine-meshed 3D VTEM inversion model resembles the contacts between different geological formations. These formations can be subdivided according to their electrical resistivity. The "blue" zone includes values above 500 Ohm m and marks the contact between the kimberlite and granodiorite. The "green-yellow" zone covers the interval between 500 and 50 Ohm m and is consistent with known kimberlite; finally the "red" zone combines all material of less than 50 Ohm m in resistivity and constitutes the top

conductive layer of sediments and lake water. The latter is consistent with previous studies.

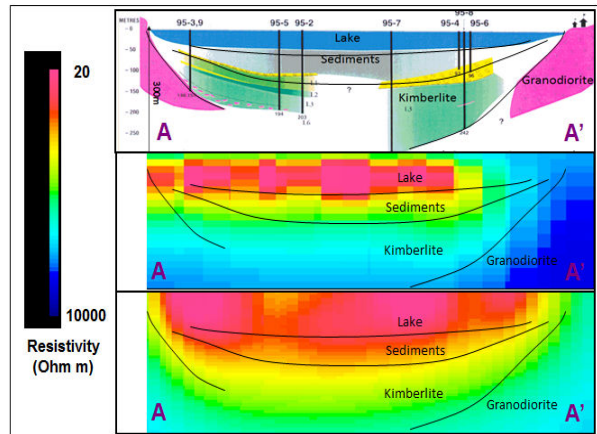


Figure 6. VTEM 3D inversion results compared to known geology. From above to below: lithological cross-section (Kretchmar, 1995); conductivities from coarse 3D VTEM inversion; conductivities from refined 3D VTEM inversion.

3D INVERSION OF ZTEM DATA

The ZTEM survey data were inverted using MTZ3D, which can invert MT, ZTEM and combined inversions over 3D structures with topography.

The 3D unconstrained ZTEM inversion was performed on a decimated data set, which accommodated 10,169 ZTEM stations, sampled at 6 frequencies (30 to 720 Hz) and recorded for 4 components (real and imaginary X-tipper and Y-tipper). Please refer to (Vozoff, 1972; Berdichevsky, 2003) for details on tipper transfer functions. The total number of data was therefore 244,056. The data were inverted on a 874,800 cell mesh with smallest cells discretized to 50x50x25 m measure. The inversion has converged to 2.29×10^6 in 20 iterations showing good overall data fit (see figure 7).

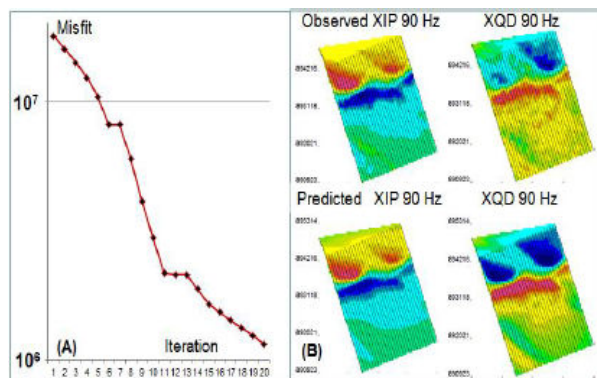


Figure 7. ZTEM 3D inversion convergence and data fit. (a): Convergence curve; (b): Observed X-tipper (real and imaginary at 90 Hz) compared to predicted equivalents. **NOTE: UBC-GIF uses standard MT coordinate system and defines tipper transfer function in Weise sense (Wiese, 1965; Parkinson, 1959; Berdichevsky, 2003), which is not consistent with their tipper and coordinate convention.**

The results of the ZTEM inversion were compared with the geology as well as with the conductivity models recovered using 3D VTEM inversions. Furthermore, the results were supported by previously carried out 2D inversions of ZTEM data (Kaminski and Legault, 2010) using Zvert2d, a Geotech in-house software for inverse modelling. In figure 8 a selected profile positioned directly over the kimberlite is subjected to comparative analysis showing similarities and differences in recovered geo-electrical properties to the depth of 800m.

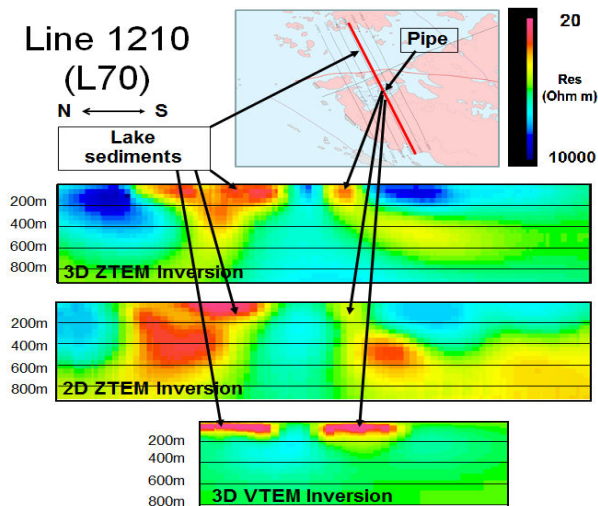


Figure 8. Comparison of three conductivity models cross-sectioned at ZTEM line 1210 (VTEM line 70). Top to bottom: 3D ZTEM inversion (UBC-GIF); 2D ZTEM inversion (Geotech); 3D VTEM inversion (UBC-GIF).

The areal coverage of ZTEM survey is greater than that of the VTEM survey, however there are clear similarities. Both show the conductive signature of known structures and electrical conductivities from the inversions are with the same numerical range.

CONCLUSIONS

The comparative analysis carried out for three independent conductivity models, acquired without a-priori constraints, shows great similarities. The conductive lake sediments are clearly delineated in all 3 inversions. The kimberlite pipe is clearly outlined and coincides with its mapped positioning. The main differences include the signatures of deep-seated structures, which can be only seen in ZTEM inversions. This can be attributed to the fact that ZTEM, as a natural plane wave source EM system, has greater penetration depth. Other differences are between the 2D and 3D ZTEM inversion models. In general, the 3D model (UBC) shows greater conductivity contrast. Another advantage of using the 3D code is the recovery of a more vertically confined sedimentary layer, which has been known to reach no more than 150m in thickness.

Figure 9 shows the 3D distribution of electrical conductivity recovered by ZTEM 3D inversion (UBC) compared to interpolated 2D results (Geotech). The geometry of the structure recovered by the 3D code is a more accurate model of the kimberlite, which shows the transition from more conductive crater facies to consolidated (less conductive) diatreme. Validity of this transition is yet to be confirmed.

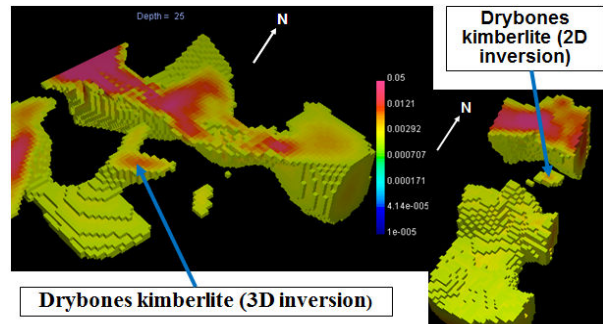


Figure 9. 3D distribution of electrical conductivity, truncated at 500 Ohm m, showing the transition from crater facies to the diatreme in case with 3D ZTEM inversion (UBC-GIF).

In conclusion, the study confirms that using airborne natural source EM surveying is an effective technology for kimberlite exploration and perhaps one of very few airborne EM techniques, which may be capable of delineating electrical property variations in resistive domain. The latter may be extremely important for exploration of non-magnetic kimberlites with weathered crater facies and mainly composed of consolidated material. Such targets are extremely challenging for conventional EM/Mag combination and in some estimates may number up to 25% of total kimberlites occurring within the Canadian Shield (Kaminski et al, 2010).

REFERENCES

- Berdichevsky, M. N., Dmitriev, V., Golubtsova, N., Mershchikova, N., Pushkarev, P., 2003, Magnetovariational Soundings: New Possibilities., *Physics of Solid Earth*, 3, 3-30.
- Dunn, C.E., Smith, D., Kerr, D.E., 2001, Biogeochemical survey of the Drybones Bay area, NWT using outer bark of black spruce. Geological Survey of Canada, Open File 3919.
- Kaminski, V., Legault, J.M, Kumar, H. (2010) The Drybones kimberlite: a cast study of VTEM and ZTEM airborne EM results, 21ST ASEG International Geophysical Conference and Exhibition, Extended Abstract. Sydney, Australia, 22-25 August 2010, 4 pp.
- Kretschmar, U., 1995, Drill Report on the Drybones Bay Kimberlite Property, Drybones Bay, Great Slave Lake, District of MacKenzie, Northwest Territories, Canada.
- Li Y., Oldenburg D. W., 1996, 3-D inversion of magnetic data. *Geophysics* 61, 394-408.
- Oldenburg, D. W., Haber, E., Shekhtman, R., 2011, Three dimensional inversion of multi-source time domain electromagnetic data, Submitted to *Geophysics*, May 2011, 41p.
- Parkinson, W.D., 1959, Direction of rapid geomagnetic fluctuations, *Geophys. J. R. Astron. Soc.*, 2, 1-14.
- Vozoff, K., 1972, The Magnetotelluric Method in the Exploration of Sedimentary Basins, *Geophysics*, 37, 1, 98-141.
- Wiese, H., 1962, Geomagnetische Tiefentellurik XI Die streichrichtung der untergrundstrukturen des elektrischen widerstandes, entschlossen aus geomagnetischen variationen, *Geofis. Pura.*, 52, 45, 303 (published in German).